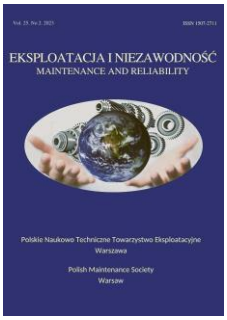

Eksploatacja i Niezawodnosc – Maintenance and Reliability
Volume 28 (2026), Issue 4
journal homepage: http://www.ein.org.pl

Article citation info:
Nowak R, Stachyra G, Pieńczuk P, Gmitrzuk M, Śniadkowski M, Experimental vibration analysis of pilot night vision goggles in the context of exploitation in helicopters, Eksploatacja i Niezawodnosc – Maintenance and Reliability 2026: 28(4) http://doi.org/10.17531/ein/218866

Experimental vibration analysis of pilot night vision goggles in the context of exploitation in helicopters

Indexed by: Web of Science Group

Radosław Nowak[a,*], Grzegorz Stachyra[b,c], Paweł Pieńczuk[c,d], Michał Gmitrzuk[e], Mariusz Śniadkowski[b]

[a] Department of Automotive Engineering, Mechatronics and Mechanics, Faculty of Automotive and Construction Machinery Engineering, Warsaw University of Techonology, Poland
[b] Department of Teaching Methods and Techniques, Faculty of Mathematics and Information Technology, Lublin University of Technology, Poland
[c] PCO S.A., Polska Grupa Zbrojeniowa (Polish Armaments Group), Warsaw, Poland
[d] The Institute of Micromechanics and Photonics, Faculty of Mechatronics, Warsaw University of Technology, Poland
[e] Material Engineering Laboratory, The Military Institute of Armoured and Automotive Technology, Sulejówek n. Warsaw, Poland

Highlights

- Experimental testing of helicopter pilot night vision goggles.
- Dynamic behaviour of the NVG during harmonic excitation.
- Military standards range of excitations extension.
- Internal structural integrity testing of the NVG.
- Exploitation of the NVG in the helicopter cabin in dynamic conditions.

Abstract

Helicopter pilots operate in a vibratory environment that substantially exceeds that of fixed-wing aircraft, creating stringent demands for the durability and dynamic stability of head-supported equipment. This study presents an experimental investigation of the vibration behaviour of prototype helicopter pilot goggles tested on an electrodynamic exciter over a frequency range exceeding applicable defence standards. The aim was to verify assembly integrity, assess the short-term strength of load-bearing components, identify natural frequencies of the goggle system, and generate reference data for future finite-element model validation. Sinusoidal excitations up to 20 g were applied to a steel mounting plate, a dedicated holder, and the complete goggle assembly in two extreme optical-track configurations. Acceleration and displacement responses were recorded using Bruel & Kjær accelerometers and processed through custom software to obtain amplitude–frequency characteristics and resonance peaks. The results indicate significant amplification of vibration in selected structural regions, particularly within the 50–250 Hz and 450–500 Hz bands, corresponding to natural modes of both the holder and the goggles. These findings confirm the sensitivity of the system to vibratory in-puts comparable to those encountered in helicopter cockpits and provide a validated experimental basis for subsequent high-fidelity numerical modelling and design optimisation.

Keywords
pilot goggles, night vision systems, structural dynamics, vibration testing, exploitation in helicopter

1. Introduction

Helicopter operations are characterised by a complex vibratory and acoustic environment generated primarily by the main and tail rotors, transmission system, and engine. These excitations are transmitted through the airframe into the cockpit, where they affect both pilot comfort and operational performance. Numerous studies have shown that helicopter pilots are

(*) Corresponding author.
E-mail addresses: R. Nowak (ORCID: 0000-0002-8066-7782) radoslaw.nowak@pw.edu.pl, G. Stachyra (ORCID: 0000-0002-3994-1268) g.stachyra@pollub.pl, P. Pieńczuk (ORCID: 0000-0001-8902-4022) pawel.pienczuk2.dokt@pw.edu.pl, M. Gmitrzuk (ORCID: 0000-0002-7490-1093) michal.gmitrzuk@witpis.pl, M. Śniadkowski (ORCID: 0000-0001-7561-4224) m.sniadkowski@pollub.pl

particularly sensitive to low-frequency vibrations, which overlap with the natural resonances of the human body and can lead to discomfort, musculoskeletal disorders, and degraded task performance [1–3]. Long-term exposure to such vibrations has been associated with a high prevalence of neck and back pain among rotary-wing aircrew, especially when head-supported equipment is used [4,5].

To quantify pilot exposure more comprehensively, several authors have proposed metrics that extend beyond conventional seat-based whole-body vibration assessment. In particular, the Generalised Vibration Index integrates multiple transmission paths, including seat-transmitted loads, hand–arm vibration, foot–pedal excitation, and vibration-induced visual degradation [1,6]. These studies demonstrate that conventional ISO-based approaches may underestimate pilot exposure, especially in frequency ranges where visual and control-related vibrations dominate. The findings underline that mitigation strategies focused solely on seat isolation may overlook critical pathways affecting pilot performance and safety.

Vibration mitigation in helicopters has therefore been addressed at multiple levels. At the source, rotor balancing, tuned absorbers, and active vibration control systems have been developed to reduce vibratory loads entering the fuselage [7–9]. Structural solutions, including passive and semi-active devices, have been proposed to attenuate vibrations in flexible components such as tail booms and fuselage panels [7,10]. In parallel, significant research effort has been devoted to the reduction of helicopter cabin noise, which is closely coupled with structural vibrations. Experimental and numerical studies have identified dominant noise transmission paths through the gearbox region, firewall, and fuselage panels, with tonal components linked to rotor and engine harmonics [11,12]. Active structural acoustic control approaches, including optimisation of sensor and actuator placement, have demonstrated the potential for substantial reductions in cabin sound pressure levels and associated structural vibrations [13]. Together, these works highlight the strong interdependence between vibration and noise phenomena within the helicopter cabin environment.

At the human–machine interface, the use of helmet-mounted systems—most notably night vision goggles (NVGs)—introduces additional biomechanical and perceptual challenges. A substantial body of research has shown that NVGs increase head-supported mass, shift the centre of gravity forward, and restrict the field of view, thereby requiring larger and more frequent head movements [4,14–16]. Experimental and modelling studies consistently indicate that these altered kinematic demands, rather than mass alone, significantly increase cervical spine loading and muscle activity [3,15,16]. When combined with whole-body vibration, these effects are further amplified, leading to increased fatigue, reduced visual stability, and degraded task performance [3,17–19]. Importantly, several studies have demonstrated that helmet-mounted systems can experience vibration amplification relative to the seat, particularly in frequency ranges relevant to helicopter operation [2,3,20].

Despite extensive research on helicopter vibration, cabin noise, and the ergonomic consequences of NVG use, the dynamic behaviour of NVG assemblies themselves has received limited attention. Existing studies predominantly focus on pilot biomechanics, perception, or cabin-level vibration and noise [2,3,11,12,14,15,16], while the structural response of NVGs under representative vibratory excitation is rarely investigated. Moreover, qualification tests for such equipment are typically conducted within narrow frequency bands defined by standards [21], which may not fully capture the excitation spectrum encountered during real helicopter operations.

The present study addresses this gap by experimentally investigating the vibration behaviour of helicopter pilot night vision goggles over an extended excitation frequency range. By testing the goggles and their mounting system on an electrodynamic exciter at acceleration levels exceeding standard requirements, the study aims to identify natural frequencies, assess dynamic amplification effects, and verify structural integrity under forced vibration. The results provide essential experimental data for the validation of future finite element models and contribute to a more comprehensive understanding of NVG performance in the vibratory environment of helicopter operations.

In the case of the goggles that were tested and intended for use by helicopter pilots, a number of requirements related to structural vibrations must be met. Consequently, following the referencing of standards [21] and the extension of the excitation frequency range, it was determined that the designed and

manufactured product would be mounted and tested on an electrodynamic exciter.

The objective of the tests was to ascertain the following:

- The necessity of verification is twofold in this instance: firstly, in order to confirm the correctness of the structure's assembly; secondly, to ensure that the structure is assembled in accordance with the relevant regulations.
- The purpose of this study is to verify the temporary strength of load-bearing elements.
- The natural vibration frequency of the system was checked and the ranges of vibration modes were compared with the forced vibrations on the helicopter pilot's seat.
- The provision of input data is essential for the validation of accurate simulation models, as will be outlined in the team's forthcoming publication.

In accordance with the standard under which the tests are conducted, the frequency range of the excitation applied to the designed element is 0-500 Hz. Following a thorough evaluation, it was determined that two experiments would be conducted. These experiments are of paramount importance from both an engineering and scientific perspective, and concern the following:

- The following steps are required to verify the correctness of the mounting brackets' design for the tested equipment: firstly, the frequency and amplitude of vibrations of successive elements of the test stand on the tested object must be correlated.
- The product was tested in a wider excitation frequency band than that specified in the defence standard. This was due to the fact that the frequencies occurring in the helicopter that affect the pilot may exceed the standard range and cause equipment malfunctions.

2. Materials and methods

The experimental procedure involved the utilisation of an IMV electrodynamic exciter, designated as the series J model, which was regulated by the proprietary software of the manufacturer, designated as the K2 vibration controller. Elements were attached to the upper handle of the exciter and subjected to sinusoidal vibrations with the acceleration amplitude shown in Figure 1. The maximum excitation frequency was 2000 Hz for the base plate tests and 500 Hz for the other elements. The frequency was reduced due to concerns about damage to the exciter and special holder, as the vibrations were tested in subsequent stages using an acceleration amplitude of 20g, where g is the acceleration due to gravity. This value exceeds twice the maximum specified in the defence standard. The frequency range specified in the defense standard for equipment intended for installation in helicopters is 5–500 Hz, with a maximum displacement amplitude of 2.5 mm. Due to the storage of the devices in transport cases and their shipment over long distances, the goggles are also exposed to mechanical shocks. Moreover, there is a possibility of impacts involving the goggles mounted on the helmet; therefore, the tests we conducted extend the requirements of the defense standard, particularly with respect to excitation amplitude (twice) and acceleration levels (four time).

Figure 1 presents a series of examples illustrating the relationship between accelera-tion amplitude and excitation frequency. The blue solid line from monitor 12955 refers to measurements from the main accelerometer attached to the table, operating in a feedback loop with the exciter control software. The maximum accel-eration amplitude achieved at the centre of the table is 20g, in accordance with the research assumptions.

The primary components of the goggle's body are composed of 7075 T6 aluminium alloy, with the material parameters specified in [22]. The construction of the prototype in-corporates a variety of materials, primarily optical glass, including N-LASF44, for which the material parameters can be found in [23]. The body components are milled and sub-sequently joined with high-strength 10.9 screws.

The experiment was conducted on a steel mounting plate, to which a goggle test holder was attached, and tested across the full range of excitation frequency changes.

In the final step of the test, measurements were taken on the device mounted on the holder. Two extreme positions of the optical glasses were considered: maximal separation along the rail and maximal proximity.

During the experimental phase, Bruel&Kjaer accelerometers, model 4507B [24], with a sensitivity of 9.8 mV/g, were utilised, which were connected to a computer controlling the electrodynamic exciter. The data acquisition

process was executed by the exciter control software, and the accelerometers were physically connected to the measurement card via a micro BNC connector.

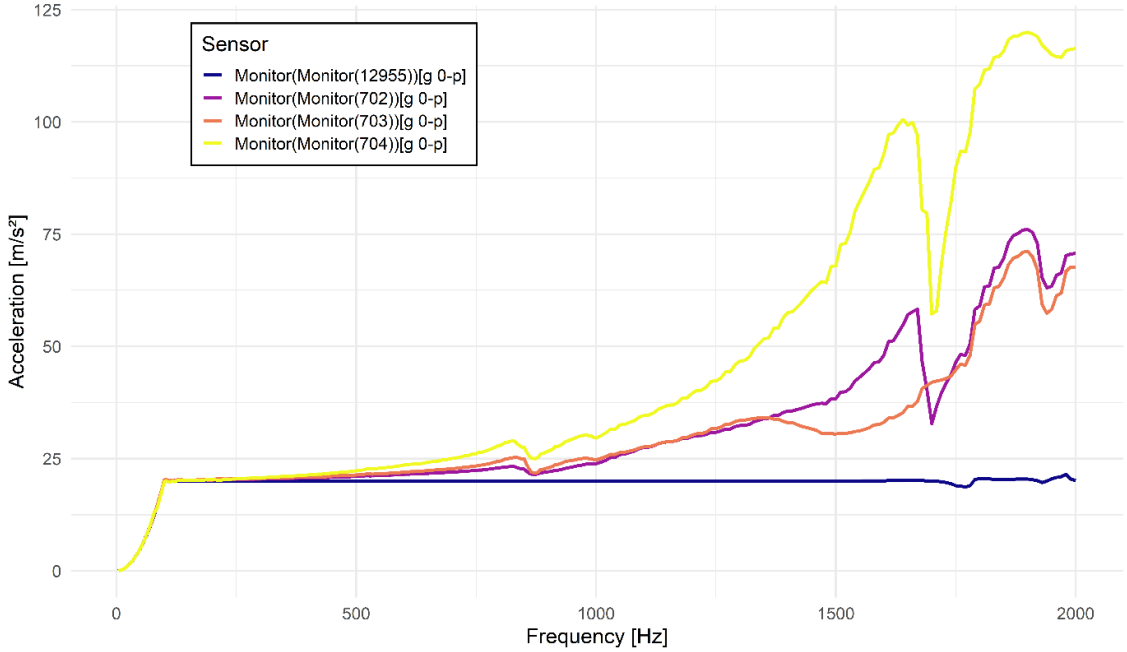

Figure 1. The amplitude waveform of the excitation generated by the exciter is depicted in blue, and the amplitude waveforms of the acceleration of three accelerometers mounted along the di-agonal from the centre of the table are shown.

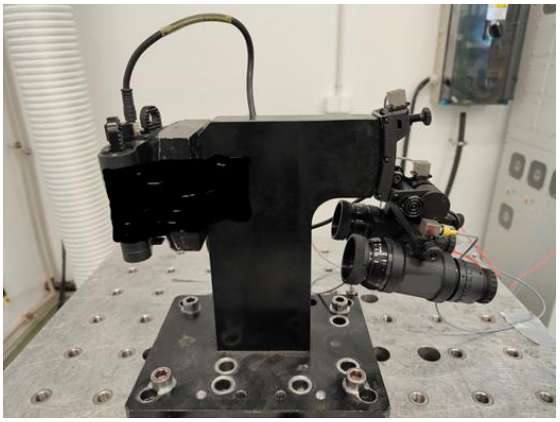

Figure 2. The following illustration depicts the night vision goggles utilised by a helicopter pilot at a test bench.

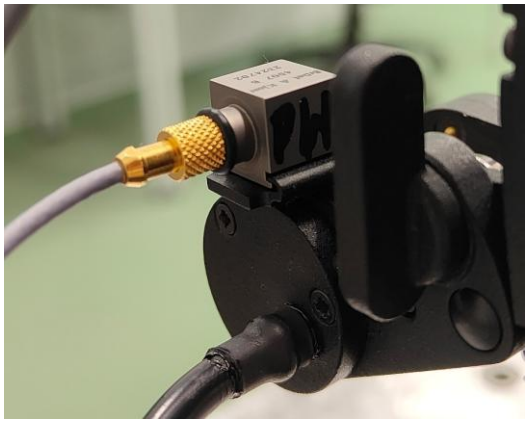

Figure 3. Accelerometers were utilised during the testing process at the designated test bench.

The data obtained from the research was processed using proprietary software developed in RStudio's integrated development environment (IDE) version 2025.05.0. The software utilised libraries such as tidyverse, ggplot2, plotly, and kableExtra. The initial step entailed the accurate importation of the data, which was subsequently converted into data frame structures for each of the measurements. These were utilised to develop amplitude-frequency characteristics for accelerations and displacements. Subsequently, the developed data sets were utilised once more to identify local maxima of accelerations and displacements. The initial 10 largest values for each characteristic were then collated into tables. In order to facilitate analysis of the characteristics, additional interactive graphs were created. The purpose of these graphs was to make it easier to read the exact points of the graphs, with local maxima occurring in the characteristics marked. The entire process was meticulously documented in the form of Rmarkdown scripts in the .Rmd format, subsequently rendered into .html files to ensure the accessibility of the developed data representation. The ensuing results are presented in the form of amplitude-frequency characteristics of acceleration or displacement.

3. Results

The results of the investigation are presented in the form of amplitude–frequency characteristics to determine the dynamic

behaviour of the tested object. The damped natural frequencies were identified, along with the corresponding acceleration and displacement amplitudes. The following subsections present the tests performed on the individual components of the measurement setup and, finally, on the helicopter pilot goggles.

3.1. Vibrations of the shaker special table

In the initial phase of the research, the vertical vibrations of a steel table affixed to the exciter head via screws were meticulously measured. It is customary for the finished components to be attached as close to the centre of the table as possible; however, the results of the vertical vibration amplitudes of the table points located along the diagonal were found to be of interest. The results of the vibration analysis of the mounting plate will be used to determine the possibility of amplitude multiplication in the goggle components in the event of resonance frequencies overlapping. Furthermore, it was intriguing to observe the impact of harmonic excitation on the vibration amplitude of a plate designed specifically for testing on an electrodynamic exciter (see Figure 4).

The measurement of accelerations was conducted by means of four accelerometers, designated 12955 (reference), and three measuring accelerometers (702, 703, 704). The accelerometers were positioned in the centre of the plate (12955) and on the diagonal of the plate – the remaining accelerometers.

Figure 4. The test station is constituted by an IMV J series electrodynamic exciter, with components mounted on the head. The presence of a special plate and goggles mounted on the holder is also evident.

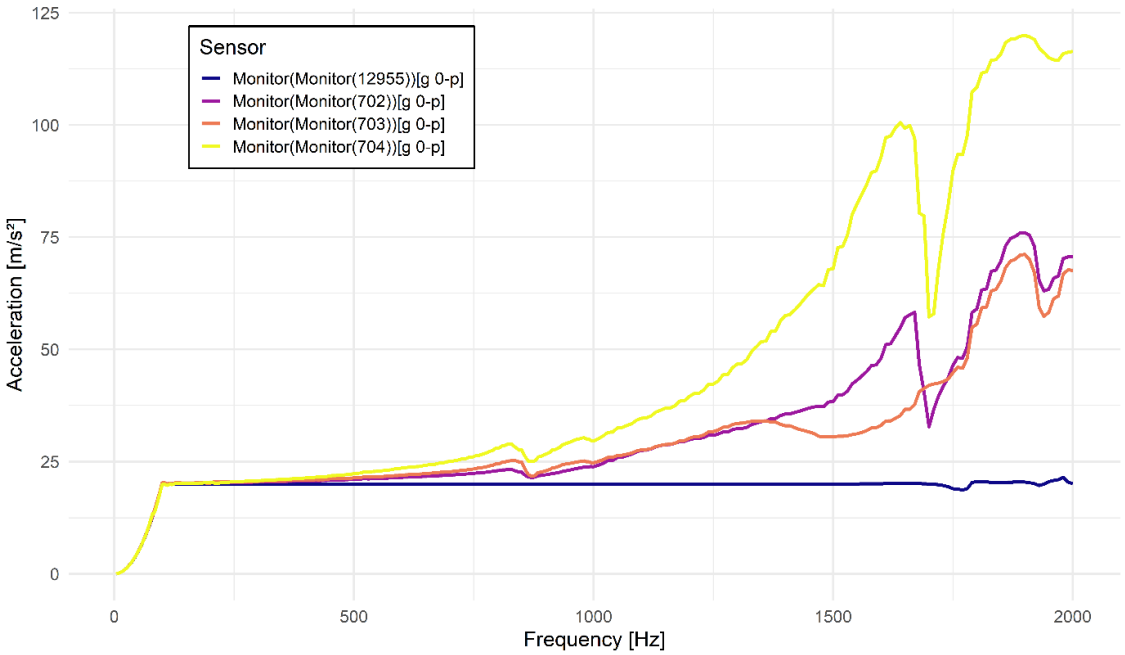

Figure 5. Amplitude-frequency characteristics of acceleration measured at four points on the mounting plate.

The acceleration measured by the 12955 accelerometer, which operated in a feedback loop with the exciter control software, was maintained at a constant set level of 20g, expressed in m/s^2. Slight changes in the acceleration values, ranging from 1610 to 1980 Hz, are evident and are the result of the superposition of the excitation frequency with the natural vibration frequency of the plate.

As demonstrated in Figure 6, the displacement amplitude graph is shown in the excitation frequency range of 0-2000 Hz. Initial large table displacements are observable, which subsequently decrease to 0.002728 mm due to the technical limitations of the electrodynamic exciter and the maintenance of a constant excitation force above 100 Hz. Despite the minimal displacement values of the table centre (as measured by sensor (12955)), the displacement amplitudes of the table corners are more than three times greater, reaching 0.01863 mm at a frequency of 1610 Hz.

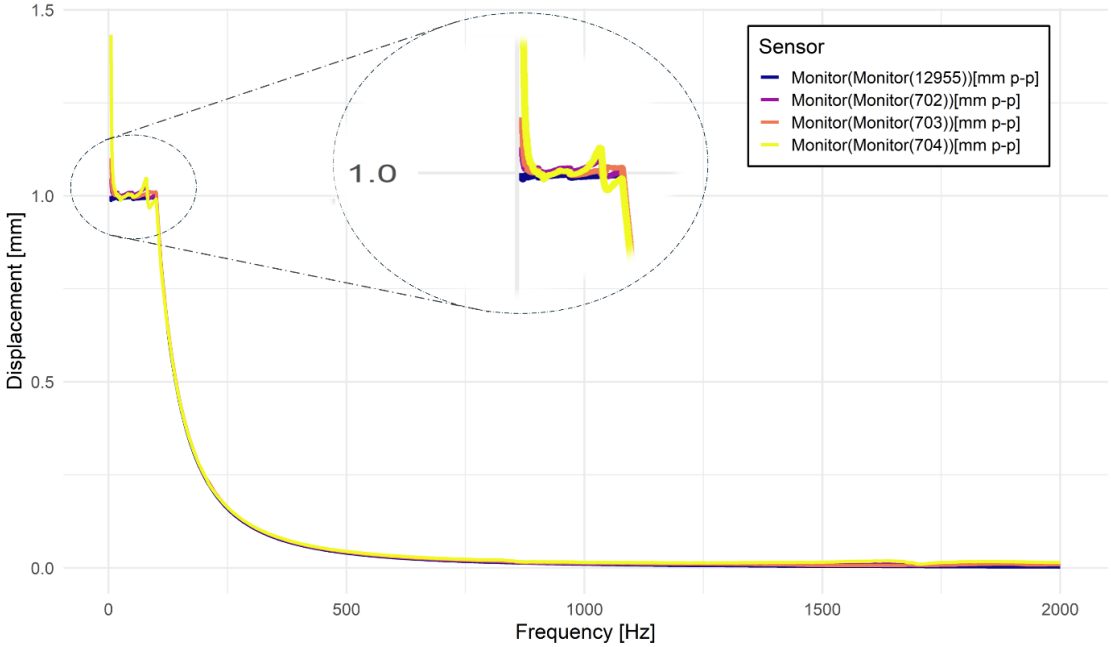

Figure 6. Amplitude-frequency characteristics of displacement at selected points on the special plate.

As illustrated in Table 1, the maximum accelerations achieved for the three accelerometers mounted on the diagonal of the plate are presented. These measurements are taken from the centre to the outer edge of the plate.

Table 1. Ten highest acceleration amplitude values of the table points.

Sensor	Resonance Frequency [Hz]	Peak Value [m/s²]
Monitor(Monitor(704))[g 0-p]	1900	119.95083
Monitor(Monitor(704))[g 0-p]	1640	100.50974
Monitor(Monitor(704))[g 0-p]	1760	93.41707
Monitor(Monitor(702))[g 0-p]	1900	76.01045
Monitor(Monitor(703))[g 0-p]	1900	71.20721
Monitor(Monitor(703))[g 0-p]	1990	67.68453
Monitor(Monitor(704))[g 0-p]	1470	64.46054
Monitor(Monitor(702))[g 0-p]	1670	58.29687
Monitor(Monitor(702))[g 0-p]	1760	48.19917
Monitor(Monitor(703))[g 0-p]	1760	46.04443

Table 2. Ten largest values of table point displacement amplitude.

Sensor	Resonance Frequency [Hz]	Peak Value [mm]
Monitor(Monitor(704))[mm p-p]	5.35	1.362472
Monitor(Monitor(704))[mm p-p]	5.65	1.291215
Monitor(Monitor(704))[mm p-p]	6.45	1.174240
Monitor(Monitor(704))[mm p-p]	6.75	1.154711
Monitor(Monitor(704))[mm p-p]	7.35	1.108970
Monitor(Monitor(704))[mm p-p]	8.30	1.072640
Monitor(Monitor(704))[mm p-p]	8.60	1.064639
Monitor(Monitor(704))[mm p-p]	8.85	1.063751
Monitor(Monitor(704))[mm p-p]	9.10	1.062266
Monitor(Monitor(704))[mm p-p]	9.40	1.051764

The results of the ten largest table displacements are summarised in Table 2. The results from accelerometer 704, which was located furthest from the geometric centre of the table, are visible, which is consistent with predictions and acceleration characteristics.

3.2. Results of measurements of the special holder

The special mount shown in Figure 7 was specifically designed to hold the goggles in two correct positions: the open position, ready for operation, and the closed position – folded for transport and handling when not in use. In addition, the mount provides a functionality that allows very quick detachment of the goggles from the main body. Ensuring reliable operation of this mechanism, as well as preventing accidental disconnection under vibration exposure, was an important secondary objective of the research work.

As illustrated in Figure 7, the intermediate element exhibits characteristics that are neither wholly goggles nor a helicopter pilot's helmet. The goggles are mounted on a detachable holder, which is visible in the centre of the photograph. For the purposes of the research, accelerometers were mounted on special pads in order to determine the acceleration and displacement as a function of the excitation frequency.

As illustrated in Figure 8, the acceleration curve at the mounting points of three accelerometers is shown. A substantial augmentation in acceleration amplitude becomes evident from a forcing value of 300 Hz, concomitant with the emergence of resonance frequencies within the 450-500 Hz range.

The amplitude-frequency characteristic displays no discernible indications of displacement amplitude increase within the 300-500 Hz frequency range, as evidenced in Figure 9.

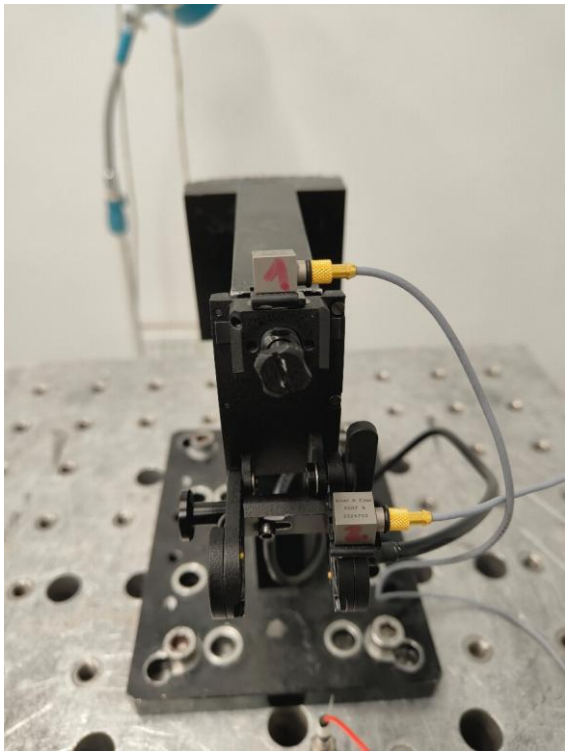

Figure 7. The helmet mount has been designed to be visible, and is equipped with accelerometers.

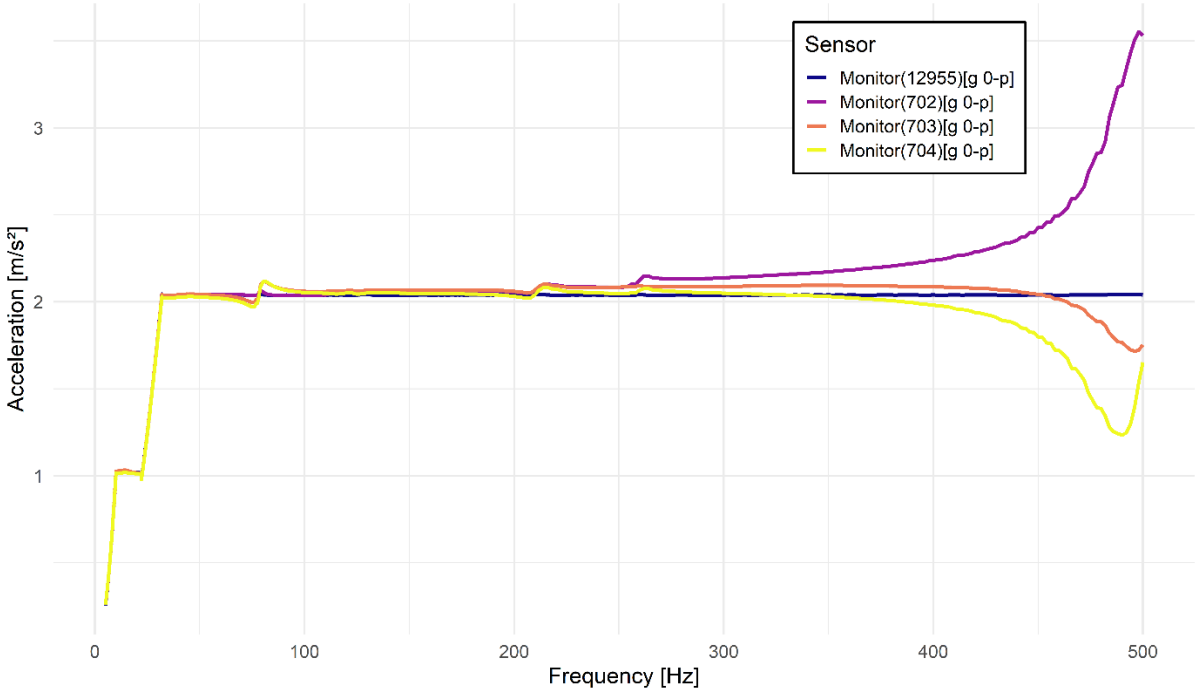

Figure 8. Acceleration curve as a function of excitation frequency.

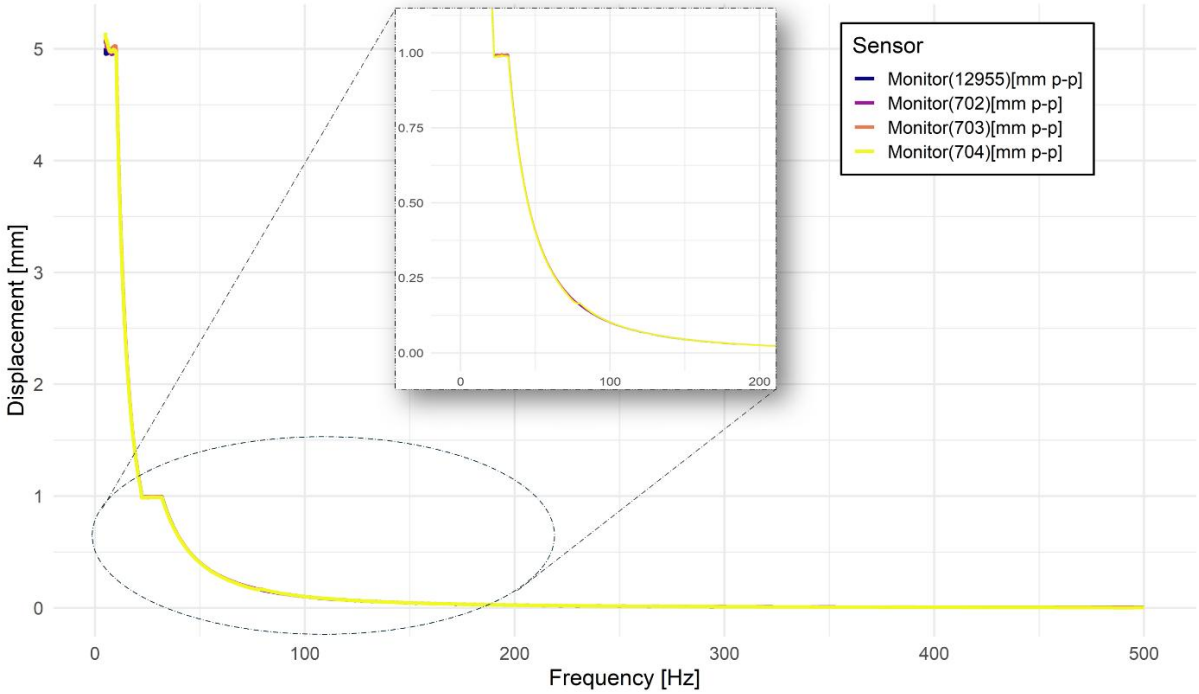

Figure 9. Amplitude-frequency characteristics of displacement.

3.3. Results obtained for the maximum adjustement set

The final phase of experimental research involved the testing of the finished product, which is intended for use by helicopter pilots. The measurement process was conducted for two extreme positions of the optical system adjustment, which has the capacity to influence the mass distribution within the system and the natural frequency.

The goggles, mounted on the stand at their maximum distance, are illustrated in Figure 10.

The accelerometers were mounted on three locations: the top of the goggle mount (702), the connection between the handle and the bridge (703), and on one of the bridge arms (704).

Figure 11 presents the acceleration curves as a function of excitation frequency. The visible data from the 12955 accelerometer correspond to vibrations in the table. Within the 50-500 Hz range, an enhancement in acceleration amplitude values becomes evident, which is associated with the emergence of the system's natural vibration frequency. This is of particular importance in the subsequent process of comparison with the excitation frequencies from the helicopter pilot's environment.

As illustrated in Figure 12, the displacement results obtained following the double integration of the acceleration values from the accelerometers are presented. A particularly salient feature is the increase in displacement amplitude in the range of 50-250 Hz in comparison to the reference table displacement.

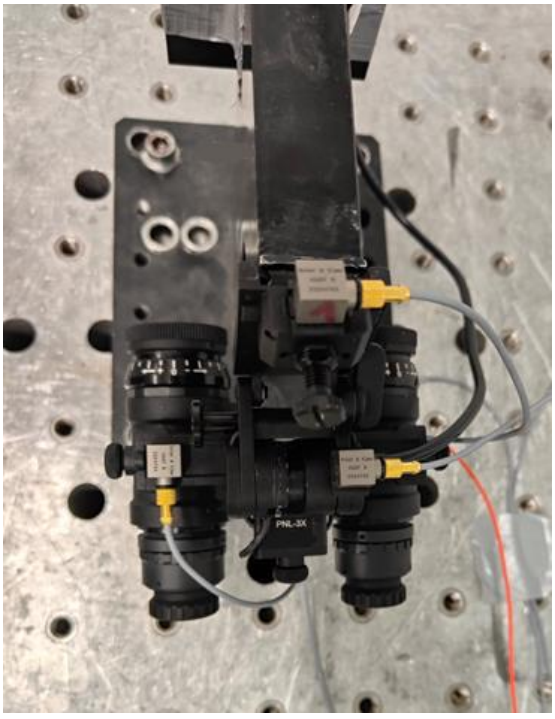

Figure 10. Night vision goggles of a helicopter pilot at a research station. Optical system set to the extreme outer position.

As illustrated in Table 3, the maximum acceleration values are predominantly associated with accelerometers (703) and (704), which were affixed to the connection between the handle and the bridge, and to the right arm of the bridge, respectively, just above the mounting of the right optical track.

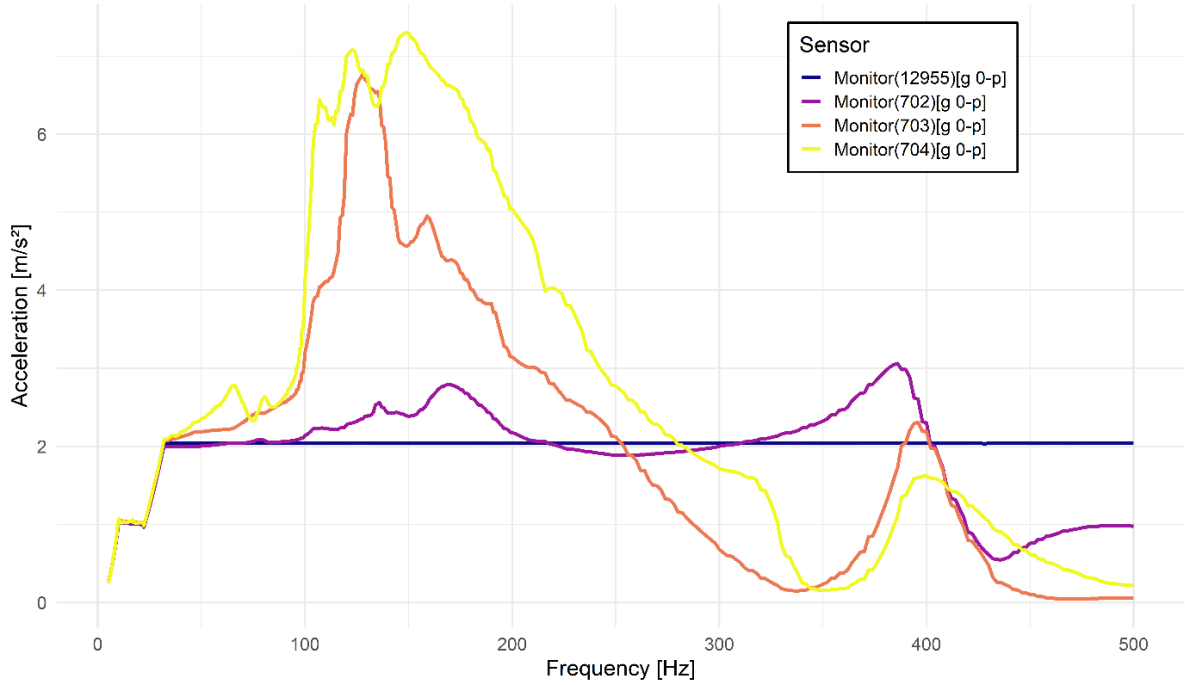

Figure 11. Amplitude-frequency characteristics of acceleration at selected points of the structure.

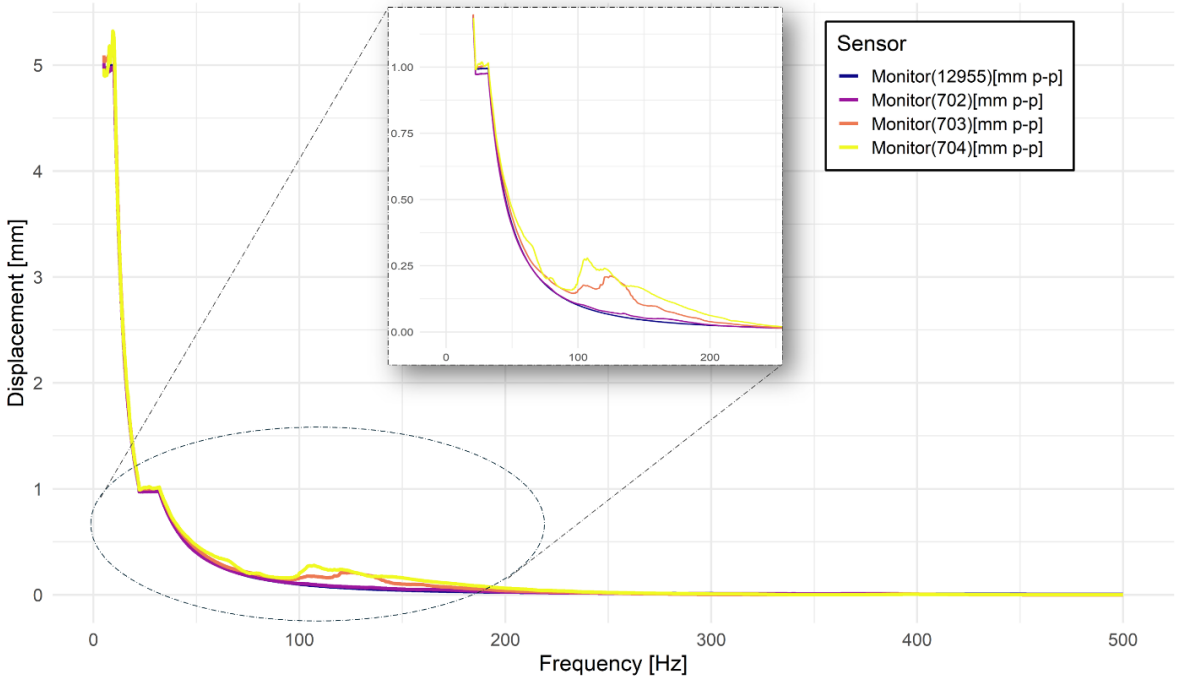

Figure 12. Amplitude-frequency characteristics of pilot goggle displacement.

Table 3. Ten highest acceleration amplitude values of the system.

Sensor	Resonance Frequency [Hz]	Peak Value [m/s²]
Monitor(704)[g 0-p]	149	7.302714
Monitor(704)[g 0-p]	123	7.079908
Monitor(704)[g 0-p]	128	6.819781
Monitor(703)[g 0-p]	128	6.773171
Monitor(703)[g 0-p]	133	6.570167
Monitor(704)[g 0-p]	107	6.440851
Monitor(703)[g 0-p]	122	6.250426
Monitor(704)[g 0-p]	113	6.212232
Monitor(704)[g 0-p]	189	5.808308
Monitor(703)[g 0-p]	159	4.951887

3.4. Results obtained for the minimum adjustement set

In the final phase of the experiment, it was decided to test the helicopter pilot's goggles when the two optical tracks were closest to each other. The mass of the entire tested system was concentrated closer to the central plane, which affected the values of displacements and accelerations as well as the frequencies and modes of natural vibrations in dynamic tests.

As illustrated in Figure 13, the accelerometers were attached to the test object, which was a pair of goggles designed for a helicopter pilot. In accordance with the protocol outlined in Section 3.3, all measuring instruments were mounted in the same manner.

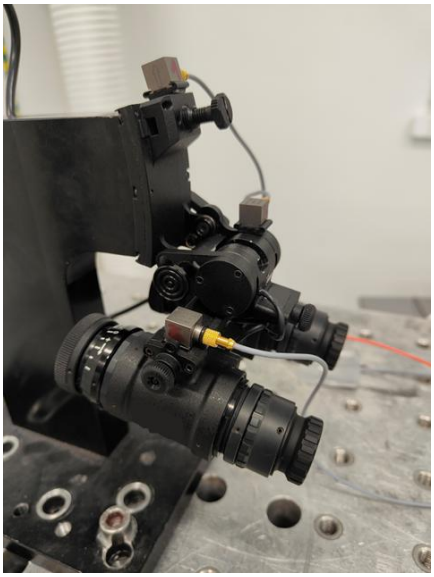

Figure 13. Placement of accelerometers on the tested object.

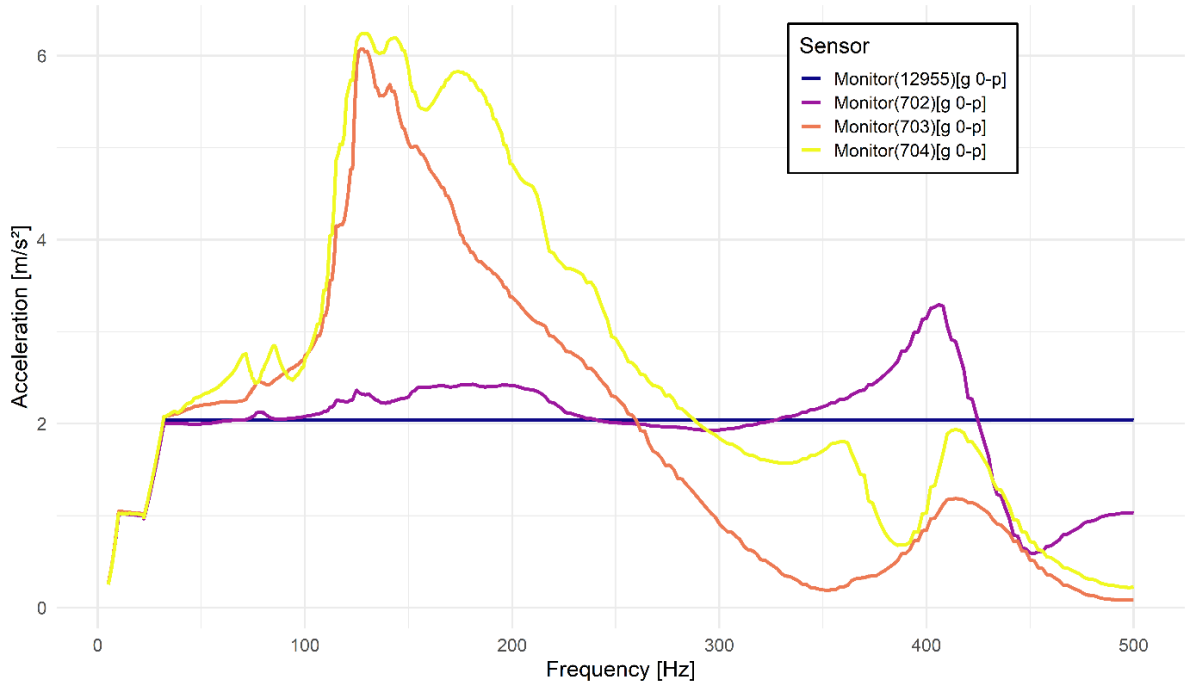

Figure 14. Amplitude-frequency characteristics of acceleration at three selected points in the system.

In the case of goggles tested with the minimum optical path distance set, decreased acceleration amplitude values in the range of 50–500 Hz are visible in Figure 14, what was expected according to the theory of mechanical vibrations.

As illustrated in Figure 15, the displacement amplitude curves are shown as a function of the excitation frequency generated by the electrodynamic exciter. In the frequency range of 50-250 Hz, an increase in displacement amplitude is observable, as measured using three accelerometers distributed on the system (see Figure 13).

Table 4. Ten highest values of the acceleration amplitude of the system.

Sensor	Resonance Frequency [Hz]	Peak Value [m/s²]
Monitor(704)[g 0-p]	128	6.243203
Monitor(703)[g 0-p]	128	6.074508
Monitor(704)[g 0-p]	137	6.033714
Monitor(704)[g 0-p]	174	5.828536
Monitor(703)[g 0-p]	141	5.685705
Monitor(704)[g 0-p]	117	5.038305
Monitor(703)[g 0-p]	154	5.014182
Monitor(703)[g 0-p]	117	4.164231
Monitor(703)[g 0-p]	185	3.760805
Monitor(704)[g 0-p]	228	3.686004

Table 5. Ten top values of the vertical deflection of the system.

Sensor	Resonance Frequency [Hz]	Peak Value [mm]
Monitor(704)[mm p-p]	9.55	5.158064
Monitor(703)[mm p-p]	9.85	5.142261
Monitor(703)[mm p-p]	7.25	5.080212
Monitor(703)[mm p-p]	6.95	5.071247
Monitor(703)[mm p-p]	6.65	5.062462
Monitor(703)[mm p-p]	6.15	5.062142
Monitor(703)[mm p-p]	5.85	5.056498
Monitor(703)[mm p-p]	5.55	5.055451
Monitor(703)[mm p-p]	5.25	5.050231
Monitor(704)[mm p-p]	8.80	5.038696

In the table 4 the maximum amplitude values recorded by accelerometers (703) and (704), mounted at the bracket–bridge interface and on the right arm of the bridge, respectively, were reported.

Table 5 presents the ten highest displacement values. It should be mentioned that they occur at relatively low excitation frequencies, yet their magnitudes are considerable in relation to the overall dimensions of the tested system.

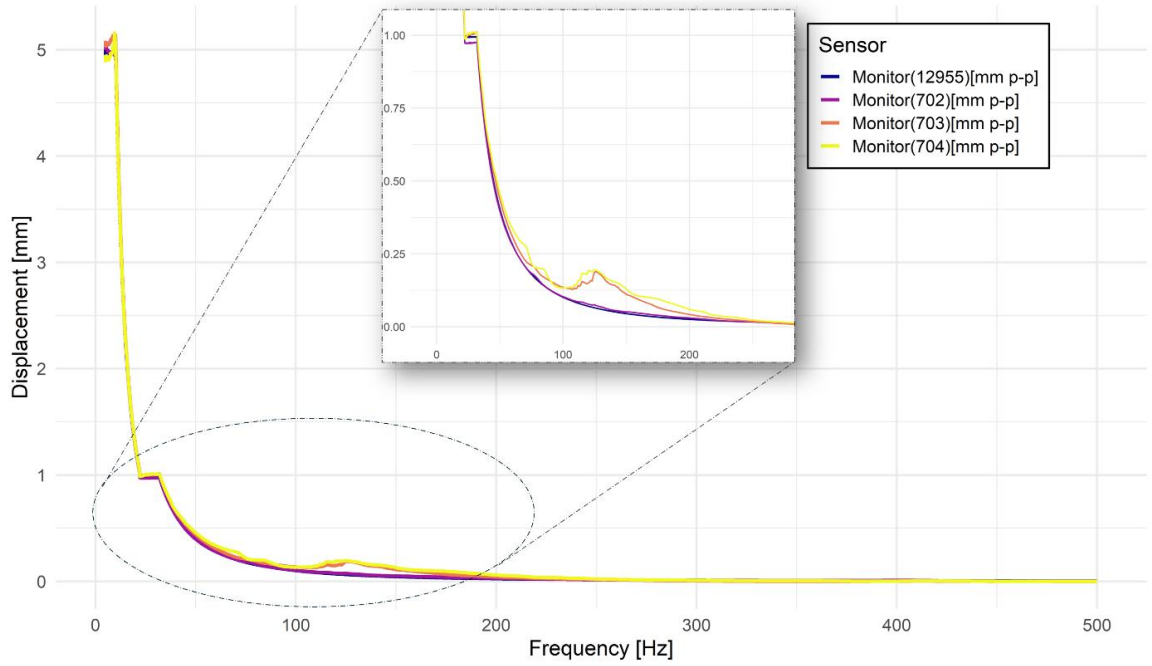

Figure 15. Amplitude-frequency characteristics of displacement.

4. Discussion and conclusion

The paper presents the results of experimental investigations of helicopter pilot night-vision goggles. The focus was placed on an aspect often overlooked during research and development activities — the dynamic excitation of the structure over a wide frequency range. Although such products are tested in accordance with the relevant military standard, the tests are typically performed within a narrow frequency band and at comparatively low amplitude levels, the acceleration amplitude of the exciter was two times higher than according to the standards.

In the present experiments, the vibration input range was extended to 0–500 Hz, which corresponds to excitations generated by helicopter equipment acting on the pilot. Additionally, the low-frequency range up to 50 Hz was investigated, as previous studies referenced in the introduction indicate potential disturbances in visual perception. Frequencies in the range of 2–8 Hz are also relevant due to their influence on internal human organs and exposure-related discomfort.

Increased acceleration and displacement amplitudes within the 50–250 Hz range may adversely affect the pilot's visual performance, which is consistent with the reviewed engineering and medical literature.

The frequency band around 400 Hz is associated with cabin noise, as well as amplitude multiplication caused by the transmission system and engine.

The amplitude–frequency characteristics reveal frequency regions where the natural vibration modes of the tested structure

are attenuated. These partially overlap with excitations generated by the drive system, which fortunately manifest predominantly as elevated noise levels rather than as excessive vibration applied to the pilot's head.

For the analysed goggles, the materials used in the construction appear to be properly selected. Despite the high acceleration amplitudes observed within 50–500 Hz and the presence of resonance frequencies (see Figures 11 and 14), the corresponding displacement amplitudes remain low (Figures 12 and 15). This indicates an appropriate selection of mounting geometry, damping characteristics of the applied materials, and the sufficiently stiff connection between the tested bracket and the night vision goggles bridge. It is worth noting that this interface is designed as a quick-release connection operable with one hand, demonstrating engineering proficiency even in the smallest detail.

The differences in results obtained for the optical channels set to the minimum and maximum possible separation distances are observed, both in terms of acceleration amplitudes and the presence of resonances. For the minimum spacing of the optical channels, the moment of inertia with respect to the longitudinal axis is lower; therefore, according to theoretical mechanics and mechanical vibrations theory, the resulting excitation moment acting on the goggle arms is reduced. This is reflected in the experimental results as lower acceleration and displacement amplitudes when the optical channels are positioned closer together, compared to the configuration with the maximum distance between optical channels.

The experimental results presented in this work — obtained over a wider excitation frequency band than specified in the standards, and at the maximum permissible acceleration of the shaker — confirm the structural correctness of the product.

The results will be used for validating finite element models, which the authors intend to present in future studies, together with a comprehensive comparison of the experimental and numerical outcomes.

References

1. Tamer A, Zanoni A, Cocco A, Masarati P. A Generalized Index for the Assessment of Helicopter Pilot Vibration Exposure. Vibration 2021; 4(1): 133–150. doi:10.3390/vibration4010012.
2. Chen Y, Ghinet S, Price A, Wickramasinghe V, Grewal A. Evaluation of Aircrew Whole-Body Vibration Exposure on a Canadian CH-147F Chinook Helicopter. Journal of the American Helicopter Society 2017; 62(2): 022004. doi:10.4050/JAHS.62.022004.
3. Law A, Wright Beatty H, Keillor J, Wickramasinghe V. Pilot Head and Neck Response to Helicopter Whole Body Vibration and Head-Supported Mass. In: Proceedings of the 73rd Annual Forum of the American Helicopter Society; 2017 May 9-11; Fort Worth, TX, USA. 2017. doi:10.4050/F-0073-2017-12044.
4. Harrison M F, Coffey B, Albert W J, Fischer S L. Night vision goggle-induced neck pain in military helicopter aircrew: a literature review. Aerospace Medicine and Human Performance 2015; 86(1): 46–55. doi:10.3357/AMHP.4027.2015.
5. O'Conor D K, Dalal S, Ramachandran V, Shivers B, Shender B S, Jones J A. Crew-Friendly Countermeasures Against Musculoskeletal Injuries in Aviation and Spaceflight. Frontiers in Physiology 2020; 11: 837. doi:10.3389/fphys.2020.00837.
6. Tamer A, Zanoni A, Cocco A, Masarati P. Generalized Measure of Vibration Exposure for Helicopter Pilots. In: Proceedings of the 45th European Rotorcraft Forum; 2019 Sep 17-20; Warsaw, Poland. Paper 154. 2019.
7. Davoodi E, Safarpour P, Pourgholi M, Foumani M S, Parvaz R, Badiei H. Evaluation of the vibration transmitted to pilot's body parts to determine the contribution of different design parameters in deficiency of available seats. International Journal on Interactive Design and Manufacturing 2022; 16(1): 339–357. doi:10.1007/s12008-021-00829-2.
8. Qi-You C, Yan Z, Zhi-Zhuang F, Quan-Long C. A Coupled Helicopter Rotor/Fuselage Dynamics Model Using Finite Element Multi-body. MATEC Web of Conferences 2016; 77: 01016. doi:10.1051/matecconf/20167701016.
9. Wu J, Ondra V, Luebker J, Kalow S, Riemenschneider J, Titurus B. Experimental Modal Analysis of a Rotating Tendon-Loaded Helicopter Blade Demonstrator. Mechanical Systems and Signal Processing 2022; 178: 109286. doi:10.1016/j.ymssp.2022.109286.
10. De Fenza A, Arena M, Lecce L. Innovative Passive Multifrequency Propeller Device for Noise and Vibration Reduction in Turboprop Fuselage. MATEC Web of Conferences 2018; 233: 00030. doi:10.1051/matecconf/201823300030.
11. Deaconu M, Cican G, Toma A-C, Drăgăşanu L I. Helicopter Inside Cabin Acoustic Evaluation: A Case Study - IAR PUMA 330. International Journal of Environmental Research and Public Health 2021; 18(18): 9716. doi:10.3390/ijerph18189716.

12. Yao D, Zhang J, Wang R, Chen C, Zhang Y, Zhao Y, Pang J. A Systematic Evaluation of Helicopter Cabin Noise: Case Study of Robinson R44 RAVEN II. Chinese Journal of Aeronautics 2025; 38(5): 103314. doi:10.1016/j.cja.2024.11.024.
13. Yuan Y, Lu Y, Sun J, Wang C. Research on the Optimal Selection Method of Sensors/Actuators in Active Structural Acoustic Control for Helicopter Based on Machine Learning. Measurement 2025; 245: 116631. doi:10.1016/j.measurement.2024.116631.
14. Barrett J M, Healey L A, Fischer S L, Callaghan J P. Cervical Spine Motion Requirements From Night Vision Goggles May Play a Greater Role in Chronic Neck Pain than Helmet Mass Properties. Human Factors: The Journal of the Human Factors and Ergonomics Society 2024; 66(2): 363–376. doi:10.1177/00187208221090689.
15. Barrett J M, McKinnon C D, Dickerson C R, Laing A C, Callaghan J P. Posture and Helmet Configuration Effects on Joint Reaction Loads in the Middle Cervical Spine. Aerospace Medicine and Human Performance 2022; 93(5): 458–466. doi:10.3357/AMHP.5830.2022.
16. Healey L A, Derouin A J, Callaghan J P, Cronin D S, Fischer S L. Night Vision Goggle and Counterweight Use Affect Neck Muscle Activity During Reciprocal Scanning. Aerospace Medicine and Human Performance 2021; 92(3): 172–181. doi:10.3357/AMHP.5673.2021.
17. Derouin A J, Law A J, Wright Beatty H, Wickramasinghe V, Fischer S L. The effects of whole-body vibration and head supported mass on performance and muscular demand. Ergonomics 2023; 66(1): 1–15. doi:10.1080/00140139.2022.2053589.
18. Beatty W, Law A, Thomas R, Yapa U S, Prigli A, Ensan M, Wickramasinghe V. Effects of Vibration Level and a Vibration Mitigating Cushion on Neck Strain Using a Human-Rated Shaker Facility. Laboratory Technical Report LTR-FRL-2016-0069. Ottawa, ON: National Research Council of Canada; 2016. doi:10.4224/23000466.
19. Tamer A, Zanoni A, Cocco A, Masarati P. A numerical study of vibration-induced instrument reading capability degradation in helicopter pilots. CEAS Aeronautical Journal 2021; 12(2): 427–440. doi:10.1007/s13272-021-00516-8.
20. Lewis C H, Griffin M J. Predicting the effects of vibration frequency and axis, and seating conditions on the reading of numeric displays. Ergonomics 1980; 23(5): 485–499. doi:10.1080/00140138008924762.
21. Military Standard NO-06-A107:2005. Sprzęt wojskowy – Ogólne wymagania techniczne, metody kontroli i badań – Metody badania odporności całkowitej na działanie czynników środowiskowych (in Polish); Ministerstwo Obrony Narodowej (Ministry of National Defence) 2005.
22. CZ Industry. 7075 Aluminum Properties, Strength and Uses [Internet]. Available from: https://pl.czyzindustry.com/info/7075-aluminum-properties-strength-and-uses-58086284.html.
23. SCHOTT AG. Optical Glass N-LASF44 [Internet]. Available from: https://www.schott.com/shop/advanced-optics/en/Optical-Glass/N-LASF44/c/glass-N-LASF44.
24. Hottinger Bruel and Kjaer (HBK). Type 4507B CCLD Accelerometer [Internet]. Available from: https://www.hbkworld.com/en/products/transducers/vibration/ccld-iepe/uniaxial/4507-b.